



U.S. DEPARTMENT OF
ENERGY

Office of
Science

DOE/SC-CM-22-003

FY 2022 Third Quarter Performance Metric: Demonstrate that Antarctic and Southern Ocean Regionally Refined Mesh (RRM) Improves Fully Coupled E3SM Simulations of Antarctic Sub-Ice-Shelf Melt Fluxes and Southern Ocean Climate

Contributing Authors: Stephen F. Price, Darin S. Comeau, Xylar S. Asay-Davis, Carolyn B. Begeman, Mark R. Petersen, and Carmela Veneziani (all Los Alamos National Laboratory).

July 2022

DISCLAIMER

This report was prepared as an account of work sponsored by the U.S. Government. Neither the United States nor any agency thereof, nor any of their employees, makes any warranty, express or implied, or assumes any legal liability or responsibility for the accuracy, completeness, or usefulness of any information, apparatus, product, or process disclosed, or represents that its use would not infringe privately owned rights. Reference herein to any specific commercial product, process, or service by trade name, trademark, manufacturer, or otherwise, does not necessarily constitute or imply its endorsement, recommendation, or favoring by the U.S. Government or any agency thereof. The views and opinions of authors expressed herein do not necessarily state or reflect those of the U.S. Government or any agency thereof.

Contents

1.0	Product Definition	1
2.0	Product Documentation	2
3.0	Detailed Results.....	5
3.1	Large-Scale Southern Ocean Climate Processes.....	5
3.2	Regional-Scale Metrics	13
	Amery Ice Shelf	13
	Amundsen and Bellinghousen Sea Region.....	16
	Filchner-Ronne Ice Shelf	19
4.0	References	22

Figures

Figure 1.	Ocean and sea ice grid cell size (km) for the SORRM configuration (top), which includes a refined region of 12-km grid cells in the Southern Ocean and Antarctic coastline (light blue), and low resolution of 60-km grid cells in the North Pacific (red).	3
Figure 2.	Antarctic ice shelves extending over ocean cavities (orange) surrounded by open ocean water (blue) for the SORRM mesh.	4
Figure 3.	Mesh detail of three regions shown on the insets in Figure 2: Pine Island and Thwaites Glaciers from the Amundsen Sea Region (top), the Amery Ice Shelf region of East Antarctica (middle), and the Filchner-Ronne Ice Shelf in the Weddell Sea region (bottom).....	4
Figure 4.	Time series of volumetric transport (Sv) through critical Southern Ocean passages with results from the standard-resolution simulation in red, the SORRM simulation in black, and the estimated range from observations in blue shading.	6
Figure 5.	Antarctic sea floor temperatures (°C) from simulations and observations (top row) and differences between models and observations (bottom row).	7
Figure 6.	Temperature bias (root-mean square error in °C) for the Southern Ocean continental shelf and for specific continental shelf regions around Antarctica.	8
Figure 7.	Antarctic sea floor salinities (PSU) from simulations and observations (top row) and differences between models and observations (bottom row).	9
Figure 8.	Salinity bias (root-mean square error in PSU) for the Southern Ocean continental shelf and for specific continental shelf regions around Antarctica.	10
Figure 9.	Temperature and salinity diagrams for the Southern Ocean from the following sources: World Ocean Atlas observations (WOA18; Boyer et al. 2018) (upper right); Southern Ocean State Estimate (SOSE; Mazloff 2010) (upper left); SORRM simulation (lower left); standard-resolution simulation (lower right)..	11
Figure 10.	Time series of area-integrated, sub-ice-shelf melt flux for all of Antarctica (top) and two large sub-regions (middle and bottom).	12

Figure 11. Temperature and salinity diagrams for the continental shelves along the East Antarctic coast, representative of Amery Ice Shelf cavity conditions, from the following sources: World Ocean Atlas observations (WOA18; Boyer et al. 2018) (upper right); Southern Ocean State Estimate (SOSE; Mazloff 2010) (upper left); SORRM simulation (lower left); standard-resolution simulation (lower right). 14

Figure 12. Modeled ocean temperatures along a transect cutting through Amery Ice Shelf (inset figure at upper right) averaged over the last 30 years of our 100-year simulations..... 15

Figure 13. Time series of area-integrated, sub-ice-shelf melt flux for the Amery Ice Shelf region of Antarctica. 15

Figure 14. Temperature and salinity diagrams for the Amundsen Sea continental shelf region, representative of Abbot Ice Shelf cavity conditions, from the following sources: World Ocean Atlas observations (WOA18; Boyer et al. 2018) (upper right); Southern Ocean State Estimate (SOSE; Mazloff 2010) (upper left); SORRM simulation (lower left); standard-resolution simulation (lower right). 17

Figure 15. Modeled ocean temperatures along a transect in the Amundsen Sea region (inset figure at upper right) averaged over the last 30 years of our 100-year simulations. 18

Figure 16. Time series of area-integrated, sub-ice-shelf melt flux for the Abbot Ice Shelf region of Antarctica..... 18

Figure 17. Temperature and salinity diagrams for the Weddell Sea continental shelf region, representative of Filchner-Ronne Ice Shelf cavity conditions, from the following sources: World Ocean Atlas observations (WOA18; Boyer et al. 2018) (upper right); Southern Ocean State Estimate (SOSE; Mazloff 2010) (upper left); SORRM simulation (lower left); standard-resolution simulation (lower right). 20

Figure 18. Modeled ocean temperatures along a transect in the Weddell Sea region, through the Filchner-Ronne Ice Shelf (inset figure at upper right) averaged over the last 30 years of our 100-year simulations..... 21

Figure 19. Time series of area-integrated, sub-ice-shelf melt flux for the Filchner-Ronne Ice Shelf region of Antarctica. 21

Figure 20. Comparison of Weddell Sea continental shelf density profiles for the standard configuration (red) and the SORRM configuration, averaged over the last 30 years of the simulations. 22

1.0 Product Definition

This report summarizes progress towards improving the representation of the Southern Ocean climate and its coupled interactions with the Antarctic ice sheet using the U.S. Department of Energy’s (DOE) Energy Exascale Earth System Model (E3SM). In particular, we focus on its Regionally Refined Mesh (RRM) capability, which allows for the placement of high spatial resolution in specific regions of the globe and lower resolution in others. The result is high-resolution model fidelity in regions of interest at a fraction of the computational cost required by a global, high-resolution model configuration. In the Southern Ocean RRM (SORRM) configuration discussed below, the Southern Ocean and sea ice around Antarctica are resolved at 12-km resolution. Moving farther away from the Antarctic coast and out of the Southern Ocean, spatial resolution in the ocean and sea ice models smoothly transitions back to that of E3SM’s standard-resolution configuration of between 30 and 60 km (Figure 1). The transition in resolution across the Southern Ocean, from non-eddying to eddy-permitting around Antarctica, is critical for improvements in the representation of oceanographic processes and ice sheet and ocean interactions that govern the exchange of heat and *freshwater between the ocean and Antarctica’s overlying ice shelves. These interactions are critical for accurate simulation of the “health” of Antarctica’s ice shelves under a changing climate. Ice shelves are important because they provide resistance to the flux of ice off of the Antarctic continent and into the ocean (often referred to as “buttressing”); ice-shelf degradation, e.g., through increased submarine melting, results in increased sea level rise from Antarctica via the dynamic connection between floating ice shelves and the grounded ice upstream (see e.g., Gudmundsson 2013, Sun et al. 2021).*

In the following sections, we further describe the details of E3SM v2 standard and RRM configurations that are designed to simulate, explore, and improve our understanding of ice shelf and ocean interactions in the Southern Ocean and around Antarctica. These novel configurations are designed to allow for ocean circulation under ice shelves within fully coupled, global simulations (described in greater detail by Comeau et al. [2022] for E3SM v1). We first provide detailed visualizations of the differences in computational meshes employed for our standard-resolution and SORRM configurations. We then provide a comparison of several important simulation outputs at the scale of the entire Southern Ocean or Antarctic continent and relative to observations in order to demonstrate that outputs from our SORRM simulations are superior to those from standard-resolution configurations. Finally, we provide a more detailed, regional-scale comparison for several key coastal regions around Antarctica, again demonstrating that outputs from the SORRM configuration are superior to those from the standard-resolution configuration.

Relative to standard-resolution E3SM configurations, we show that simulations conducted with our SORRM configuration demonstrate clear improvements in Southern Ocean processes important for controlling sub-ice-shelf melt rates, both at the whole-continent and regional scale. These improvements include: (1) large-scale volume transports, a prerequisite for accurate simulation of ocean circulation at regional scales (consistent with observations for SORRM configurations but too low and outside the range of observations for standard configurations); (2) ocean bottom temperature and salinity, important because these waters ultimately come into contact with the most sensitive parts of the ice shelves (over six important continental shelf areas, mean bias reductions using SORRM are 34% for temperature and 48% for salinity relative to using standard configurations); (3) broad, overall improvements in the representation of temperature, salinity, and density for Southern Ocean water masses critical for the

accurate modeling of sub-ice-shelf circulation (high-salinity shelf water, HSSW, which is also a critical precursor to Antarctic bottom water, AABW, a driver of global ocean circulation). These improvements combine to provide time series of Antarctic sub-ice-shelf melt rates that are stable and closer to observational-based estimates in SORRM configurations than in standard, lower-resolution configurations. This conclusion applies at the whole-Antarctic scale, at the regional scale, and at the scale of individual ice shelves.

2.0 Product Documentation

The E3SM ocean and sea ice meshes presented here include the 60-to-30km “standard-resolution” mesh and the Southern Ocean Regionally Refined Mesh or “SORRM” (Figure 1). The standard resolution is 30 km at the Equator and decreases smoothly to 60 km in mid-latitude regions and then increases again to 35 km in high-latitude regions. This design was chosen because equatorial and high-latitude dynamics require higher resolution, while it is less important at mid-latitudes. The SORRM keeps this distribution in the Pacific, the world’s largest ocean, but adds refined cells of 12 km in the Southern Ocean, and the Antarctic continental shelf, coastlines, and below the ice shelves (Figure 2). The Southern Ocean dynamics are influenced by the Atlantic meridional overturning circulation, so mid-range cells of 40 km extend throughout the Atlantic to the Arctic Ocean.

In Figure 3, we show the SORRM configuration in additional detail, with mesh detail in particular regions of interest. Each regional zoom includes details for both the standard and SORRM configurations in order to provide a qualitative comparison for the additional detail afforded by the variable-resolution SORRM configuration. At low resolution, the small ice shelves, such as Pine Island Glacier and Thwaites Glacier, only contain two or three cells each, making sub-ice-shelf ocean dynamics and resultant melt rates unrealistic. The SORRM mesh, with 12-km cells, increases the number of cells by a factor of about 10 and improves the simulation of these processes.

For both our standard and SORRM configuration, mesoscale eddies are not fully resolved everywhere, and are represented through the Gent-McWilliams (“GM”) parameterization (Gent and McWilliams 1990). This parameterization is active in lower-resolution regions where the Rossby radius is not resolved, and inactive otherwise. For the standard-resolution configuration, GM is fully active for the entire globe. In the SORRM configuration, GM is off in the Southern Ocean because the Rossby radius is resolved in the refined region. The strength of the GM parameterization is linearly “ramped” down as a function of resolution, allowing for the improved representation of heat and mass transport due to ocean eddies.

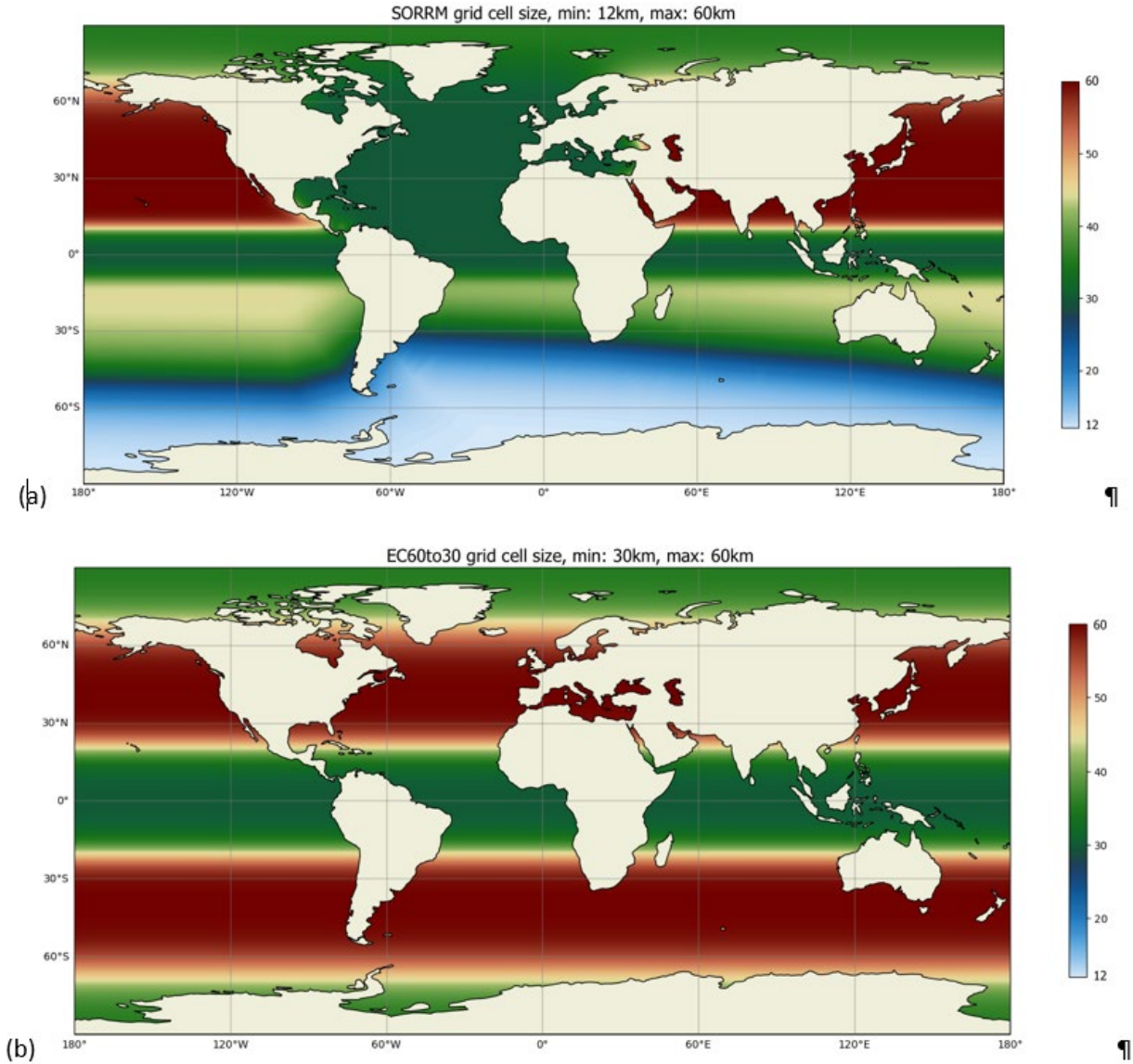


Figure 1. Ocean and sea ice grid cell size (km) for the SORRM configuration (top), which includes a refined region of 12-km grid cells in the Southern Ocean and Antarctic coastline (light blue), and low resolution of 60-km grid cells in the North Pacific (red). The standard-resolution mesh (bottom) varies between 30- and 60-km grid cells globally.

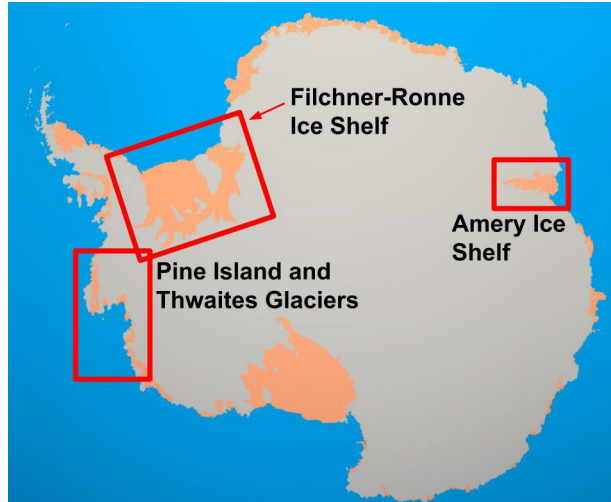


Figure 2. Antarctic ice shelves extending over ocean cavities (orange) surrounded by open ocean water (blue) for the SORRM mesh. Regions with ice-covered bedrock are shown in gray. Insets correspond to locations in Figure 3.

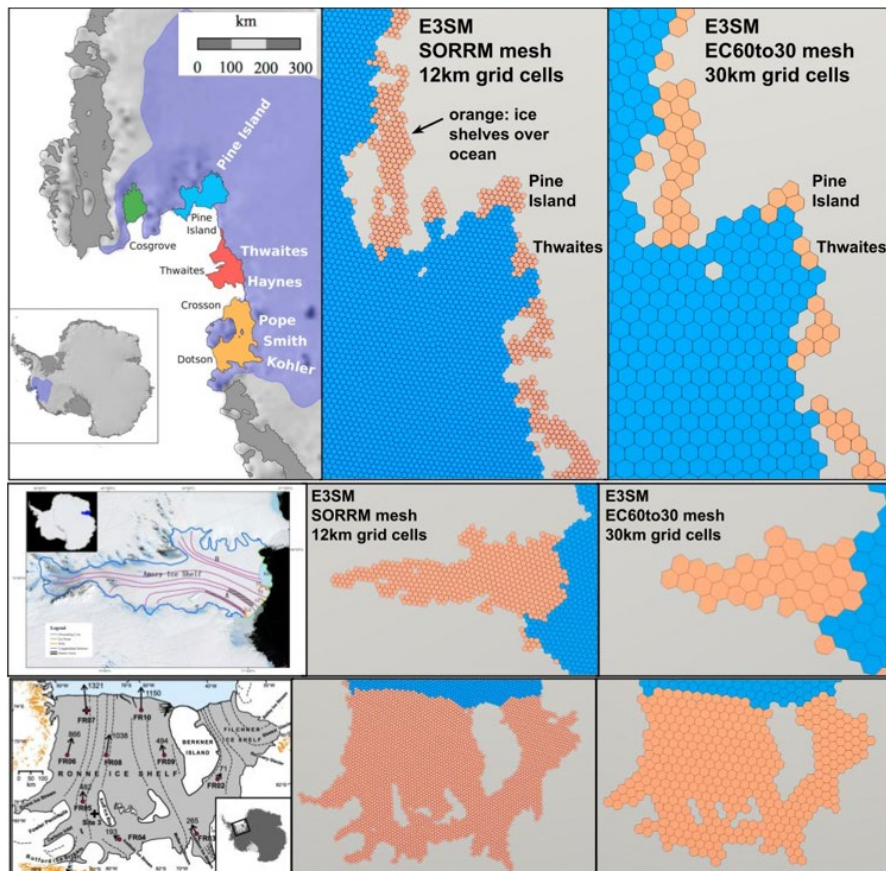


Figure 3. Mesh detail of three regions shown on the insets in Figure 2: Pine Island and Thwaites Glaciers from the Amundsen Sea Region (top), the Amery Ice Shelf region of East Antarctica (middle), and the Filchner-Ronne Ice Shelf in the Weddell Sea region (bottom). The standard mesh (right) has 30-km-wide grid cells in this region, while the SORRM mesh (middle) has 12-km cells. Reference maps (left) are from Brondex et al. (2019), Li et al. (2021), and Makinson et al. (2012).

For the simulations conducted here, both the standard and SORRM configurations were run fully coupled (active atmosphere, land, ocean, and sea ice) for 100 years under pre-industrial climate conditions. The more detailed analyses conducted below are based on the full-time series from those simulations, or climatologies constructed from the last 30 years of the simulations.

3.0 Detailed Results

A primary focus of E3SM’s Cryosphere Science Campaign is improving our understanding of how ongoing climate change will impact mass loss from the Antarctic ice sheet and hence, sea level rise. It is well understood, from both observations and modeling, that Antarctica’s floating ice shelves serve to “buttress” the flux of ice from the continent into the oceans (Scambos et al. 2004, Gudmundsson 2013, Sun et al. 2020); thinning the ice shelves (e.g., via increased melting from below) or decreasing their horizontal extent (e.g., via increased iceberg calving) decreases their capacity to resist the flow of ice from upstream. Thus, understanding the long-term “health” of ice shelves is critical for understanding how the flux of ice from Antarctica into the oceans (and hence sea level rise from Antarctica) may change in the future. Currently, approximately half of Antarctica’s mass loss to the ocean occurs via sub-ice-shelf melting (Rignot et al. 2013) and simulating this process within a global, coupled Earth system model is one of E3SM’s unique capabilities. In addition to including the relevant physical processes, its global, coupled nature ensures that important aspects of internal climate variability that impact Southern Ocean climate and sub-ice-shelf melting (Li et al. 2021) are accounted for. Further, its variable-resolution capability allows for optimizing the tradeoff between model resolution and computational cost by focusing resolution in the Southern Ocean and around Antarctica. E3SM is thus an ideal tool for better understanding how Antarctic ice shelf health may change in the future as a function of changing climate.

Through several more detailed studies (see, e.g., Jeong et al. 2020, Comeau et al. 2022, Hoffman et al. 2022) we have learned that accurate simulation of Antarctic sub-ice-shelf melt rates is complex and relies on a range of Southern Ocean climate processes, from large-scale to regional and local in nature. Below, we demonstrate the importance of adequate spatial resolution in representing these processes, and in doing so, also demonstrate the importance of E3SM’s variable-resolution capability. We first demonstrate how regionally mesh refinement improves a number of large-scale aspects of Southern Ocean climate that are important for accurate simulation of sub-ice-shelf melt rates. We then provide similar analyses at smaller scales, focusing on three very different but equally important regions that are broadly representative of the different types of ice shelf melting found around Antarctica today.

3.1 Large-Scale Southern Ocean Climate Processes

In this section, we compare the representation of the following large-scale Southern Ocean climate processes and features against observations using both our standard-resolution and SORRM model configurations:

1. Large-scale Southern Ocean transport
2. Temperature and salinity at the ocean bottom
3. Temperature, salinity, and density for the full ocean column
4. Sub-ice-shelf melt fluxes.

Figure 3 shows Southern Ocean volume transports (Sv) through two critical passages for which observations exist, the Drake Passage and the Tasmania-Antarctica Passage. In both plots, the range of values representative of present-day observations is shown by the blue-shaded region and the model time series from the standard and SORRM configurations are shown as the red and black lines, respectively. In both cases, the SORRM configuration outputs fall within, or very close to, the range expected from observations and appear approximately stable after the first 50 years of simulation. Conversely, the outputs from the standard configuration show a steady, near-linear decrease throughout the simulation, falling outside of the range of observations by 100 years (too low), and show no obvious indication of reaching a stable state. The accurate volume of these throughflows is a good indication that the Antarctic Circumpolar Current (ACC), the defining large-scale oceanographic feature of the Southern Ocean, is well represented by the SORRM configuration (and rather poorly represented by the standard-resolution configuration). In turn, an accurate representation of this large-scale circulation is an important prerequisite for an accurate model representation of various regional-scale circulations that control the flow of water on and off of the continental shelves (and hence into and out of Antarctic ice shelf cavities (Russell et al. 2018).

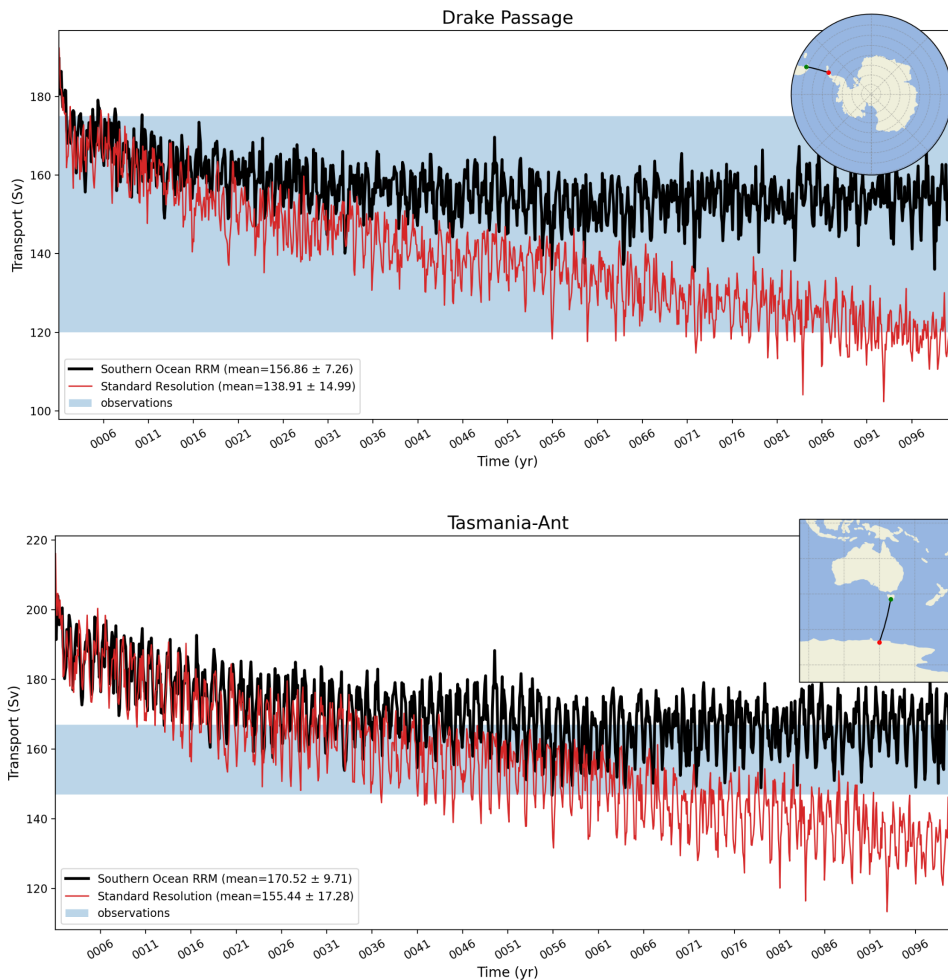


Figure 4. Time series of volumetric transport (Sv) through critical Southern Ocean passages with results from the standard-resolution simulation in red, the SORRM simulation in black, and the estimated range from observations in blue shading. Drake Passage transport is shown at the top, Tasmania-Antarctic passage transport at the bottom.

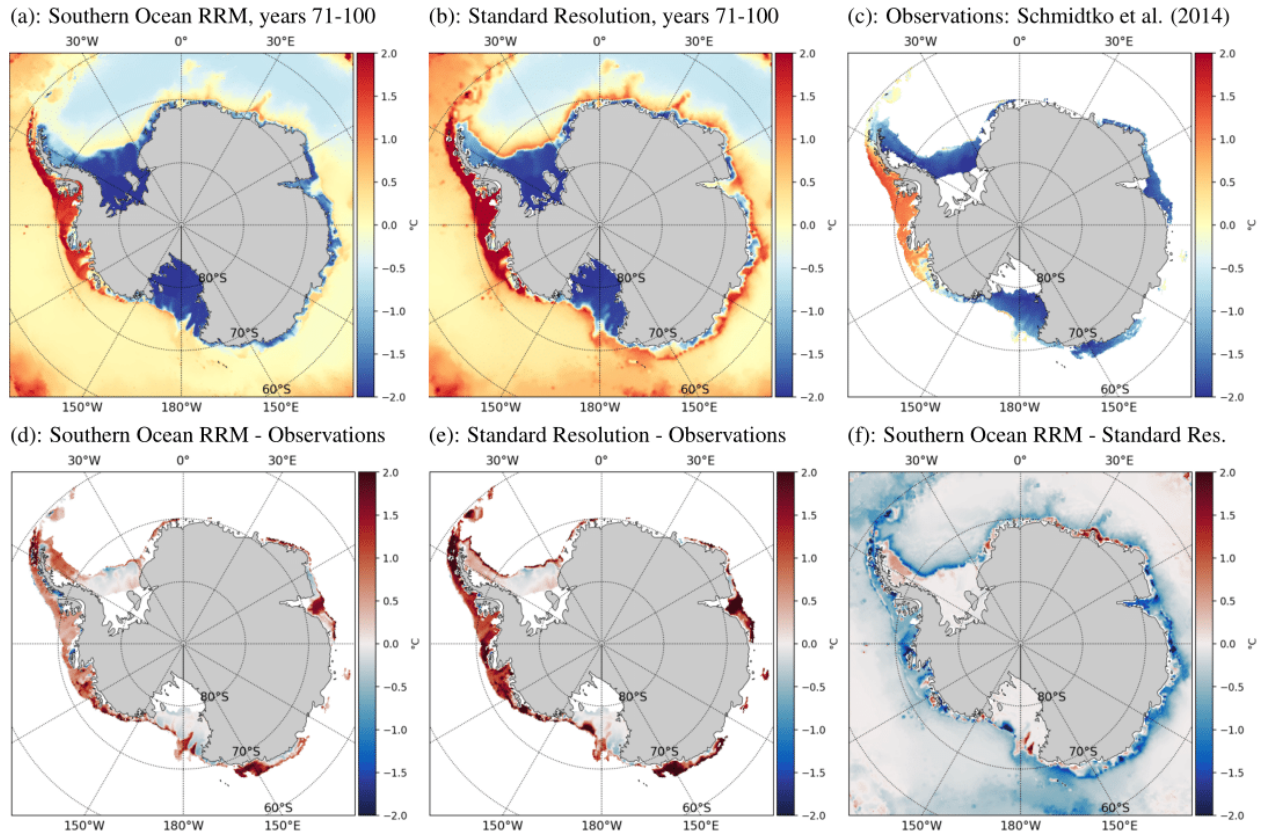


Figure 5. Antarctic sea floor temperatures ($^{\circ}\text{C}$) from simulations and observations (top row) and differences between models and observations (bottom row). In all cases, simulation values are time averages from the last 30 years of 100-year simulations. Individual panels show: temperatures from SORRM (upper left), standard resolution (upper middle), observations (upper right, from Schmidtko et al. 2014), difference between SORRM and observations (lower left), difference between standard resolution and observations (lower middle), and differences between SORRM and standard resolution (lower right).

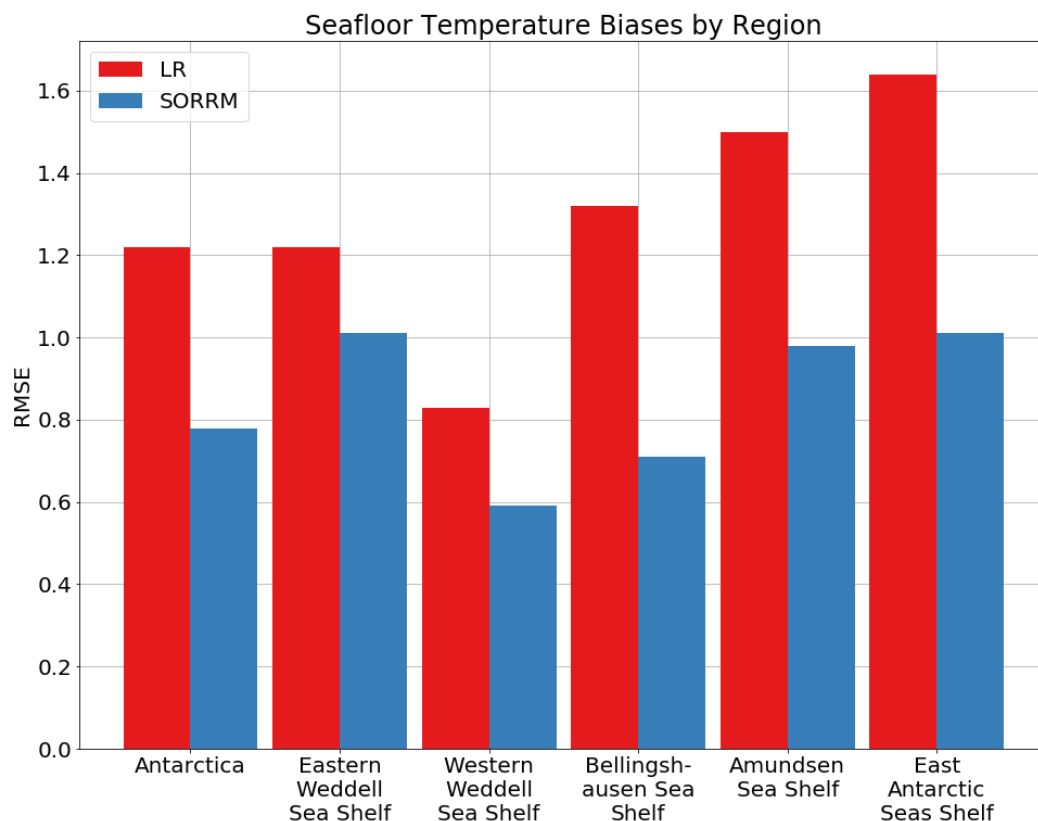


Figure 6. Temperature bias (root-mean square error in $^{\circ}\text{C}$) for the Southern Ocean continental shelf and for specific continental shelf regions around Antarctica.

In Figure 4, we show modeled ocean bottom temperatures around Antarctica and compare them to continental shelf observations from Schmitdtko et al. (2014). These are critical to model with reasonably high accuracy because they represent the temperature of the ocean waters that ultimately interact with the ice shelf grounding line and ice shelf base; according to both the observations and model outputs (top panel of Figure 4), we expect higher sub-ice-shelf melt rates for ice shelves along the Amundsen and Bellingshausen Sea coast relative to those beneath Antarctica’s larger Filchner-Ronne and Amery ice shelves (see Figures 2 and 3 for shelf locations), and this is in line with observations (Rignot et al. 2013). While both models overestimate ocean bottom temperatures with respect to observations, biases from our SORRM configuration are substantially smaller (bottom panel of Figure 4), most likely due to the improved representation of the Antarctic Slope Front (ASF) at higher resolution (Veneziani et al. 2019). The ASF mediates access of warm off-shelf waters onto the continental shelf and into the ice shelf cavities (Thompson et al. 2018). Figure 5 provides a more quantitative demonstration of the bias reduction afforded by the SORRM configuration relative to the standard configuration.

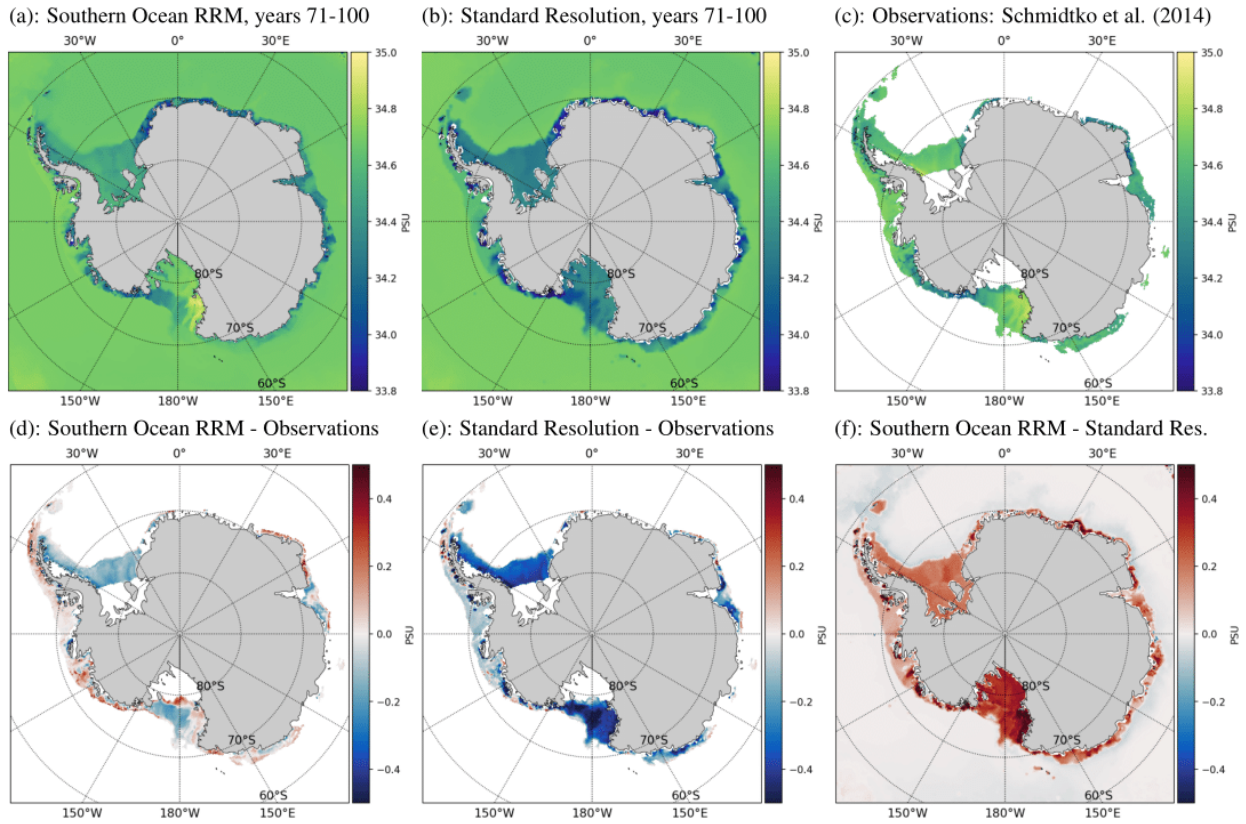


Figure 7. Antarctic sea floor salinities (PSU) from simulations and observations (top row) and differences between models and observations (bottom row). In all cases, simulation values are time averages from the last 30 years of our 100-year simulations. Individual panels show: temperatures from SORRM (upper left), standard resolution (upper middle), observations (upper right, from Schmittko et al. 2014), difference between SORRM and observations (lower left), difference between standard resolution and observations (lower middle), and difference between SORRM and standard resolution (lower right).

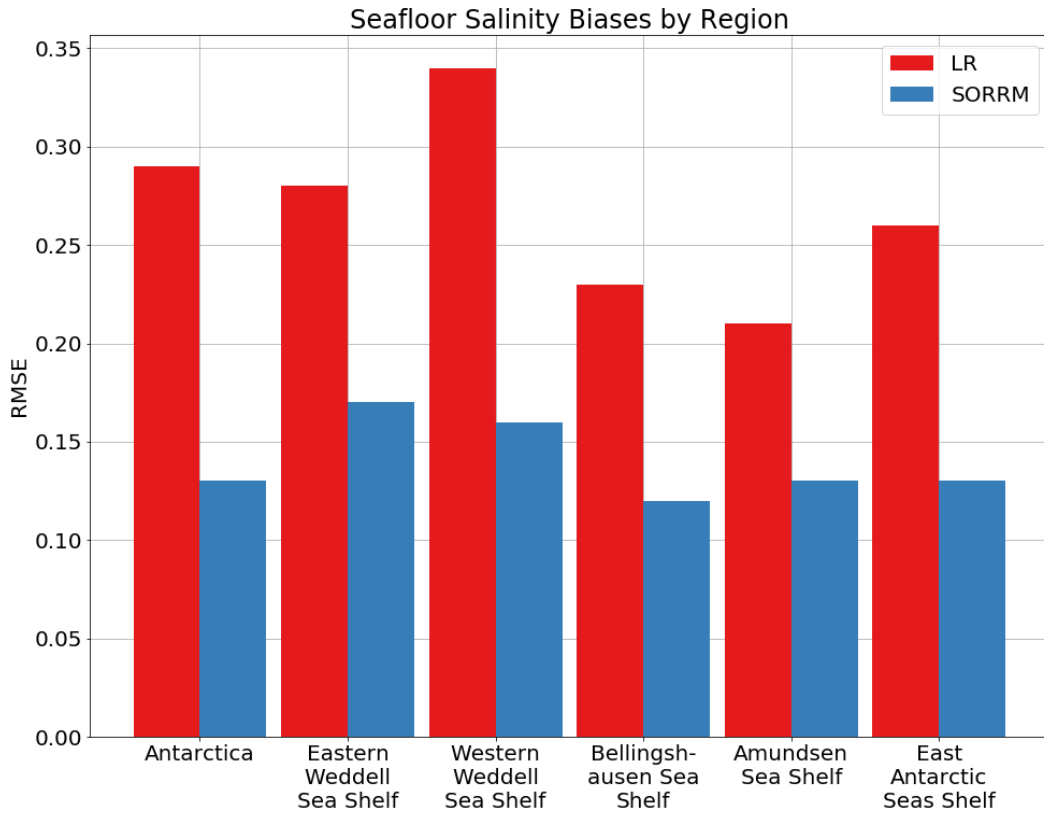


Figure 8. Salinity bias (root-mean square error in PSU) for the Southern Ocean continental shelf and for specific continental shelf regions around Antarctica.

Similar to Figure 4, Figure 6 shows ocean bottom salinities around Antarctica compared to continental shelf observations from Schmitzko et al. (2014) (top panel). Simulations with the SORRM configuration show a greatly improved representation of ocean bottom salinities relative to the standard configuration, for which salinities are much too fresh (bottom panel). For temperatures near to the freezing point, as is the case for most Southern Ocean water masses, the primary control on ocean density is salinity. Important aspects of sub-ice-shelf circulation and regional circulation are controlled by the densification and sinking of cold, saline waters around Antarctica, which are also the intermediaries to the formation of the most cold, dense water in the world's oceans, Antarctic Bottom Water, an important driver of global, thermohaline circulation (Talley 2011). Thus, the greatly reduced salinity biases shown in Figure 6 and afforded by the SORRM configuration (further quantified in Figure 7) are important not only for the correct simulation of Southern Ocean climate but the global climate as well.

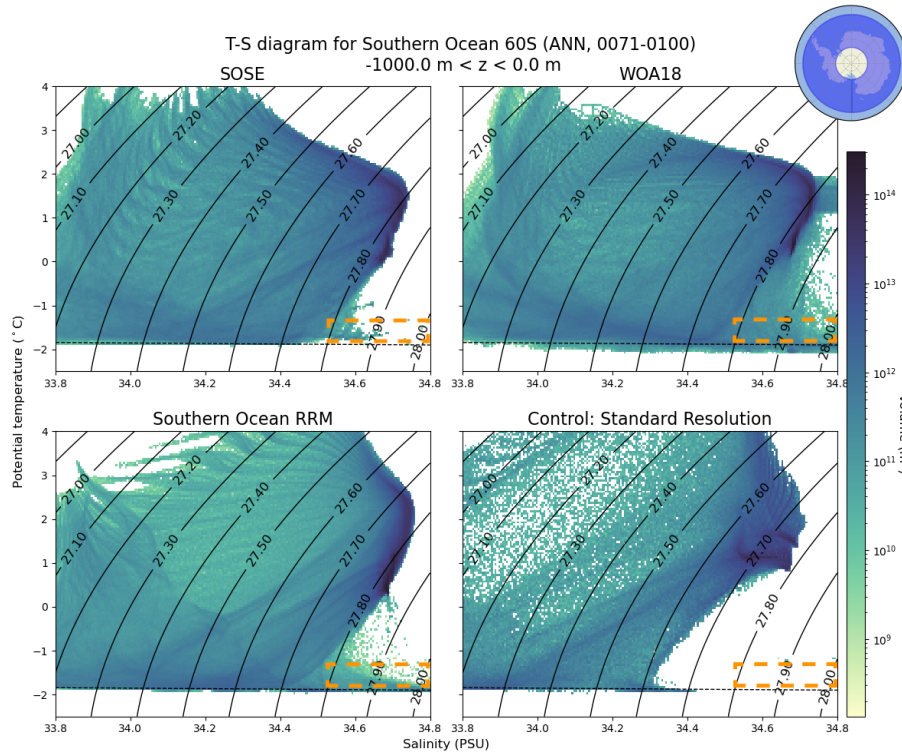


Figure 9. Temperature and salinity diagrams for the Southern Ocean from the following sources: World Ocean Atlas observations (WOA18; Boyer et al. 2018) (upper right); Southern Ocean State Estimate (SOSE; Mazloff 2010) (upper left); SORRM simulation (lower left); standard-resolution simulation (lower right). For the E3SM simulations, results are averaged over the last 30 years of a 100-year simulation. The orange dashed box marks the region in temperature, salinity, and density space representative of high-salinity shelf water (HSSW).

Temperature and salinity diagrams like Figure 8 are a concise way of summarizing and comparing ocean temperature, salinity, and density data over large regions and at all depths. In these plots, temperature on the vertical axis is plotted against salinity on the horizontal axis, the combination of which places parcels of water in their unique density space, represented by contours. In Figure 8, observations from the World Ocean Atlas (Boyer et al. 2018) are shown in the upper right and output from a data-assimilating, reanalysis-forced ocean model are shown at upper left (SOSE; Mazloff et al. 2010). In the lower row, outputs from our fully coupled SORRM (lower left) and standard configuration (lower right) are shown. As might be expected, the outputs from SOSE provide an overall good match to the observations. The outputs from the SORRM configuration also provide a reasonable match to the observations and even show some improvements over SOSE. Notably the presence of cold, saline, dense waters (high-salinity shelf water; HSSW – orange dashed box in Figure 8) that are largely absent from SOSE and completely absent from the standard resolution configuration. HSSW, which is formed when particularly salty water is left behind as sea ice forms in many regions of Antarctica, is important for controlling the exchange of waters on the continental shelf (and thus within ice shelf cavities) with the deeper ocean. It is also a precursor to the formation of Antarctic Bottom Water (Talley 2011) and thus important for global ocean circulation. A lack of HSSW production is a common bias found in most lower-resolution Earth system models (Heuze et al. 2013) and, as we show in the regional focus below, a common source of problematic biases when attempting accurate and stable simulations of sub-ice-shelf melting in Antarctica.

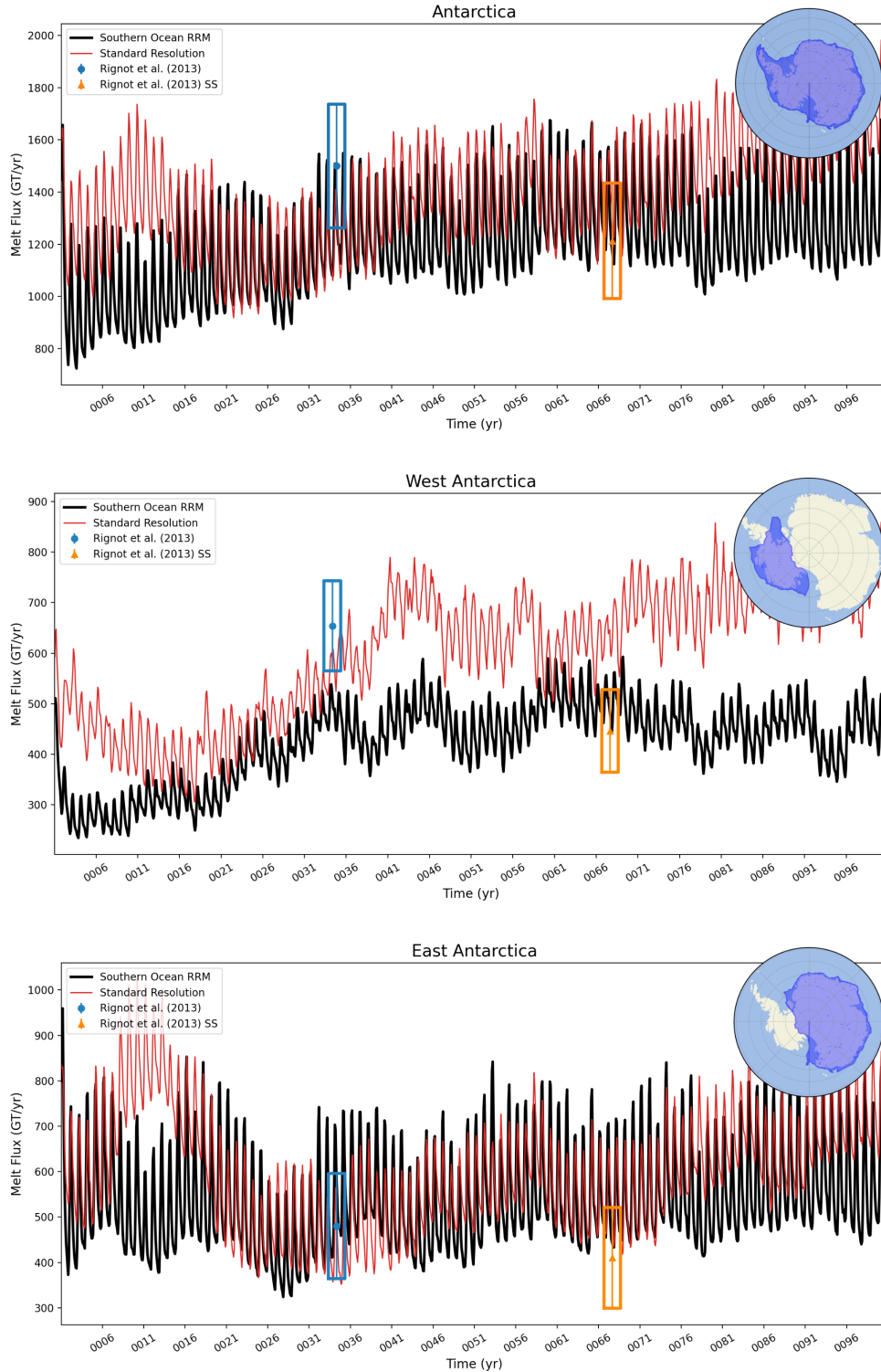


Figure 10. Time series of area-integrated, sub-ice-shelf melt flux for all of Antarctica (top) and two large sub-regions (middle and bottom). Melt fluxes from the standard-resolution and SORRM simulations are shown in red and black, respectively. The blue and orange boxes mark the span of melt rates inferred from observations of Rignot et al. (2013), with blue as an estimate for present-day and orange an estimate for pre-industrial values (the position of the box along the horizontal axis is arbitrary).

In Figure 9, we show time series of simulated sub-ice-shelf melt fluxes for all of Antarctica (top) and West (middle) and East (bottom) Antarctica, along with observationally based estimates for present-day and pre-industrial melt fluxes (blue and orange rectangles, respectively, from Rignot et al. [2013]). Because we apply pre-industrial forcing in our simulations, we aim for our simulated values to fall within the range of the orange boxes. While both simulations provide melt fluxes that look reasonable within the range of observational estimates, the simulations from the SORRM configuration (black lines) are generally more within the range of the pre-industrial estimates than those from the standard simulation (red lines). Moreover, melt fluxes from the standard configuration show a near linearly increasing trend in all regions for at least the last 40 years of the simulation, with melt fluxes from West Antarctica in particular nearly double what they should be at the end of the simulation. By contrast, melt fluxes from the SORRM configuration are more in line with pre-industrial observations and show a largely stable trend over the last several decades of the simulation.

3.2 Regional-Scale Metrics

We now illustrate how the large-scale biases and improvements discussed above impact the oceanography and sub-ice-shelf melting in three key regions. These particular regions have been chosen because they represent distinct types of ice shelf and ocean interaction that are critical for a model to be able to distinguish between and represent relatively accurately (e.g., warm and cold cavity circulation; see Thompson et al. 2019). Simultaneously, they represent regions that are problematic or challenging to model in E3SM's standard-resolution configuration (Comeau et al. 2022, Hoffman et al. 2022).

Amery Ice Shelf

In Figures 10, 11, and 12, we show regional plots of ocean temperature and salinity, horizontal and vertical transects of ocean temperatures, and time series of sub-ice-shelf melt rates that are representative of East Antarctic ice shelves and, in particular, the Amery Ice Shelf (see Figure 12). The relatively narrow continental shelf along the East Antarctic coast is problematic in standard-resolution simulations because relatively warm off-shelf waters are able to lap up onto the continental shelf and make their way into ice shelf cavities (e.g., Figure 4b). Simultaneously, fresh and warm biases on the continental shelf (Figure 6b; Figure 10) mean that the waters there are not dense enough to impede the flow of off-shelf waters onto the continental shelf and into ice shelf cavities. Amery Ice Shelf is a good example, where the dense water mass, HSSW, in the cavity is lacking in standard-resolution simulations but present in SORRM simulations (Figure 10, lower row). The result is subtle, but important: in Figure 11 we can see a region of unrealistically elevated temperatures within the Amery cavity for the standard simulation that is absent from the SORRM (and SOSE) simulation. This seemingly small difference has a dramatic impact on sub-ice-shelf melt rates; in Figure 12, sub-ice-shelf melt rates for Amery in the standard-resolution configuration are up to an order of magnitude too large. Conversely, melt rates from the SORRM configuration are much closer to the range of observations and reasonably stable.

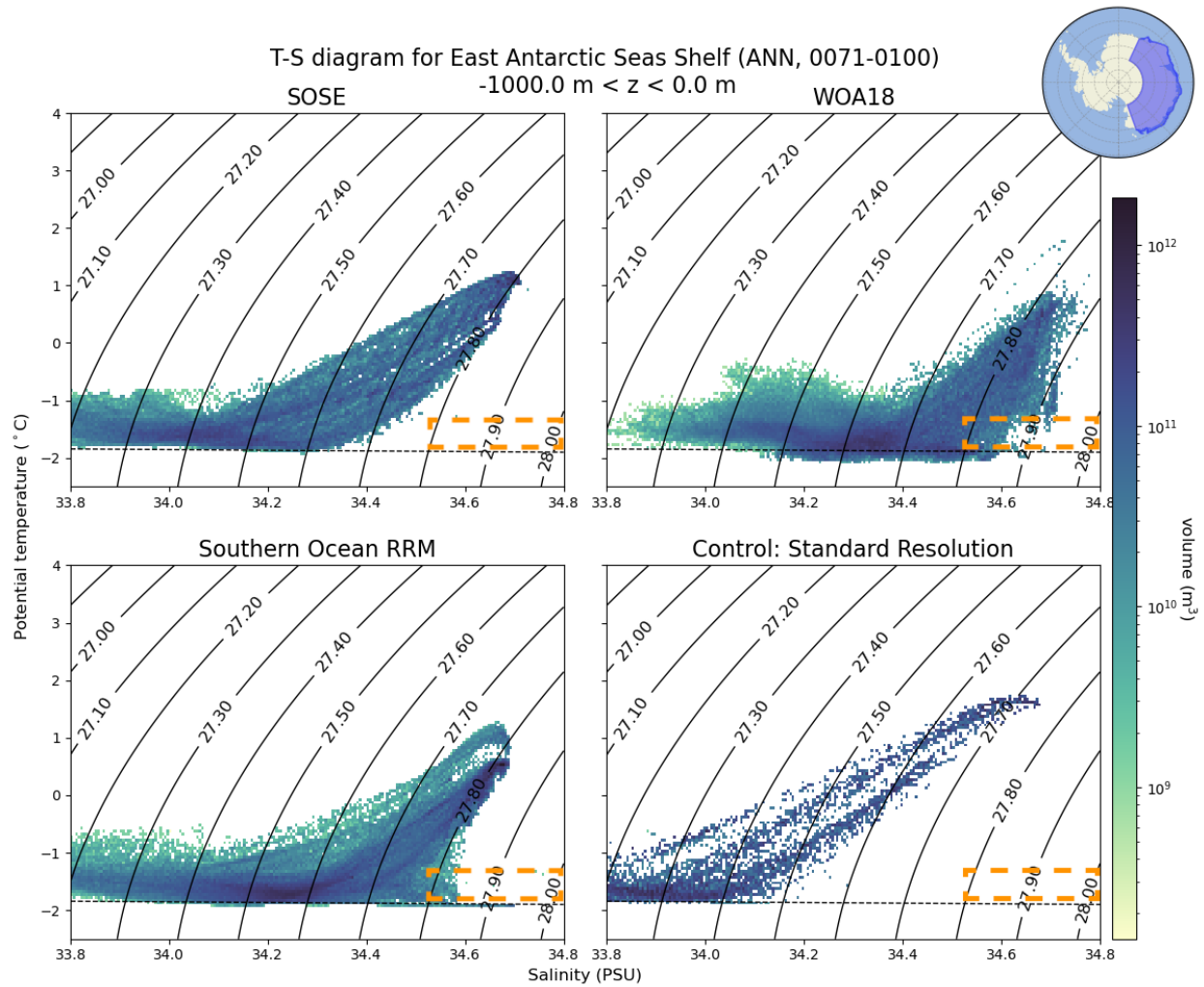


Figure 11. Temperature and salinity diagrams for the continental shelves along the East Antarctic coast, representative of Amery Ice Shelf cavity conditions, from the following sources: World Ocean Atlas observations (WOA18; Boyer et al. 2018) (upper right); Southern Ocean State Estimate (SOSE; Mazloff 2010) (upper left); SORRM simulation (lower left); standard-resolution simulation (lower right). For the E3SM simulations, results are averaged over the last 30 years of a 100-year simulation. The orange dashed box marks the region in temperature, salinity, and density space representative of high-salinity shelf water (HSSW).

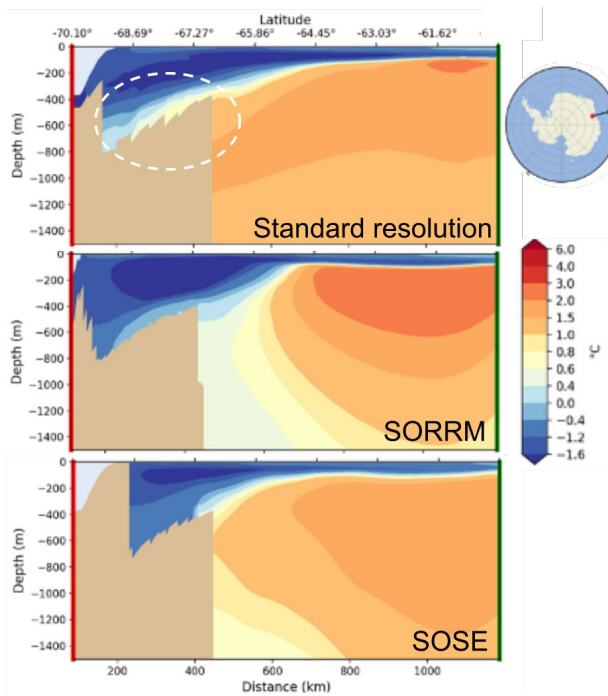


Figure 12. Modeled ocean temperatures along a transect cutting through Amery Ice Shelf (inset figure at upper right) averaged over the last 30 years of our 100-year simulations. Shown are results from E3SM’s standard configuration (top row), from the SORRM configuration (middle row), and from the Southern Ocean State Estimate (SOSE; Mazloff et al. 2010) (bottom row). The white dashed circle in the top panel indicates warm water accessing the shelf cavity that is absent from both the SORRM and SOSE model outputs.

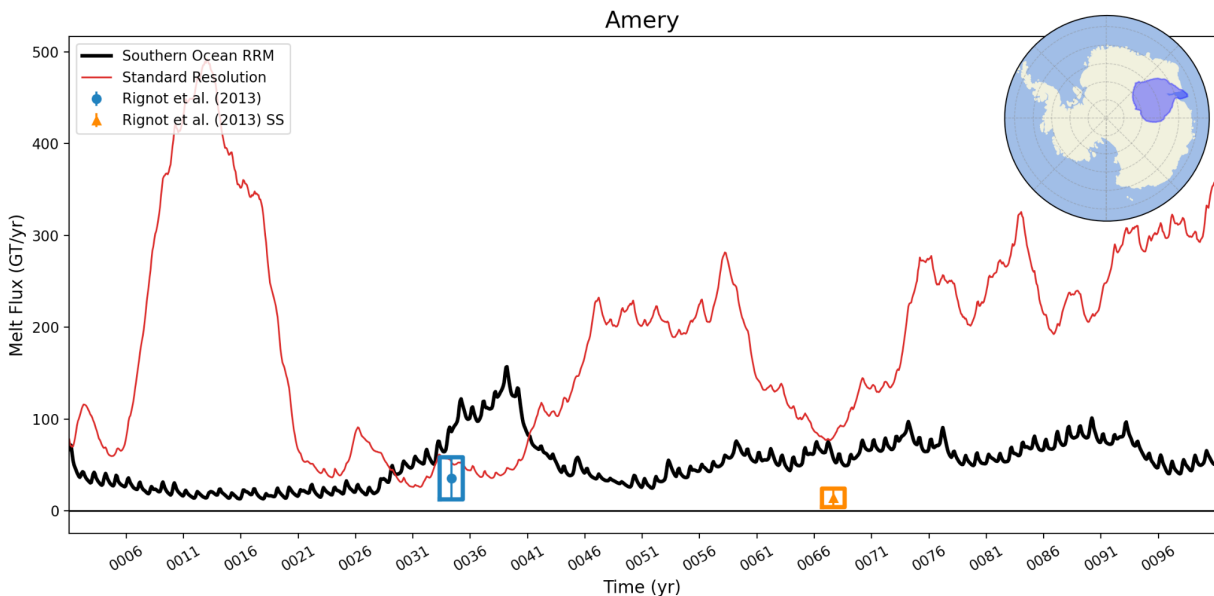


Figure 13. Time series of area-integrated, sub-ice-shelf melt flux for the Amery Ice Shelf region of Antarctica. Melt fluxes from the standard-resolution and SORRM simulations are shown in red and black, respectively. The blue and orange boxes mark the span of melt rates inferred from observations of Rignot et al. (2013), with blue as an estimate for present-day and orange an estimate for pre-industrial values (note that the position of the box along the horizontal axis is not relevant).

Amundsen and Bellinghausen Sea Region

In Figures 13, 14, and 15, we show regional plots of ocean temperature and salinity, horizontal and vertical transects of ocean temperatures, and time series of sub-ice-shelf melt rates in the Amundsen Sea region of West Antarctica (see Figure 13). This region is of particular interest because it is the region where the majority of Antarctic mass loss and sea level rise originates and the region most likely prone to marine ice sheet instability (see, e.g., Pattyn and Morlighem 2020), the primary concern for potential sudden and rapid future sea level rise from Antarctica. Currently, grounding line retreat and dynamic ice sheet mass loss from outlet glaciers in this region is caused predominantly by warm Circumpolar Deep Water (CDW) incursions into the ice shelf cavities (Dinniman et al. 2016), which result in ice shelf thinning and loss of ice shelf “buttressing” (Gudmundsson 2013). In Figure 13, we again show temperature, salinity, and density in the Amundsen Sea region from observations, SOSE reanalysis, and our standard and SORRM model configurations. In this case, SORRM outputs look as good or better than SOSE relative to the observations and markedly better than outputs from the standard configuration, which are both too warm and too fresh. Along with a large, too-warm ocean temperature bias at mid-depths (Figure 14), the result is that sub-ice-shelf melt rates in this region are up to 5x too large in the standard-resolution model after ~50 years (Figure 15). Sub-shelf melt rates from the SORRM configuration, however, remain well within the range of observational constraints throughout the duration of the 100-year simulation.

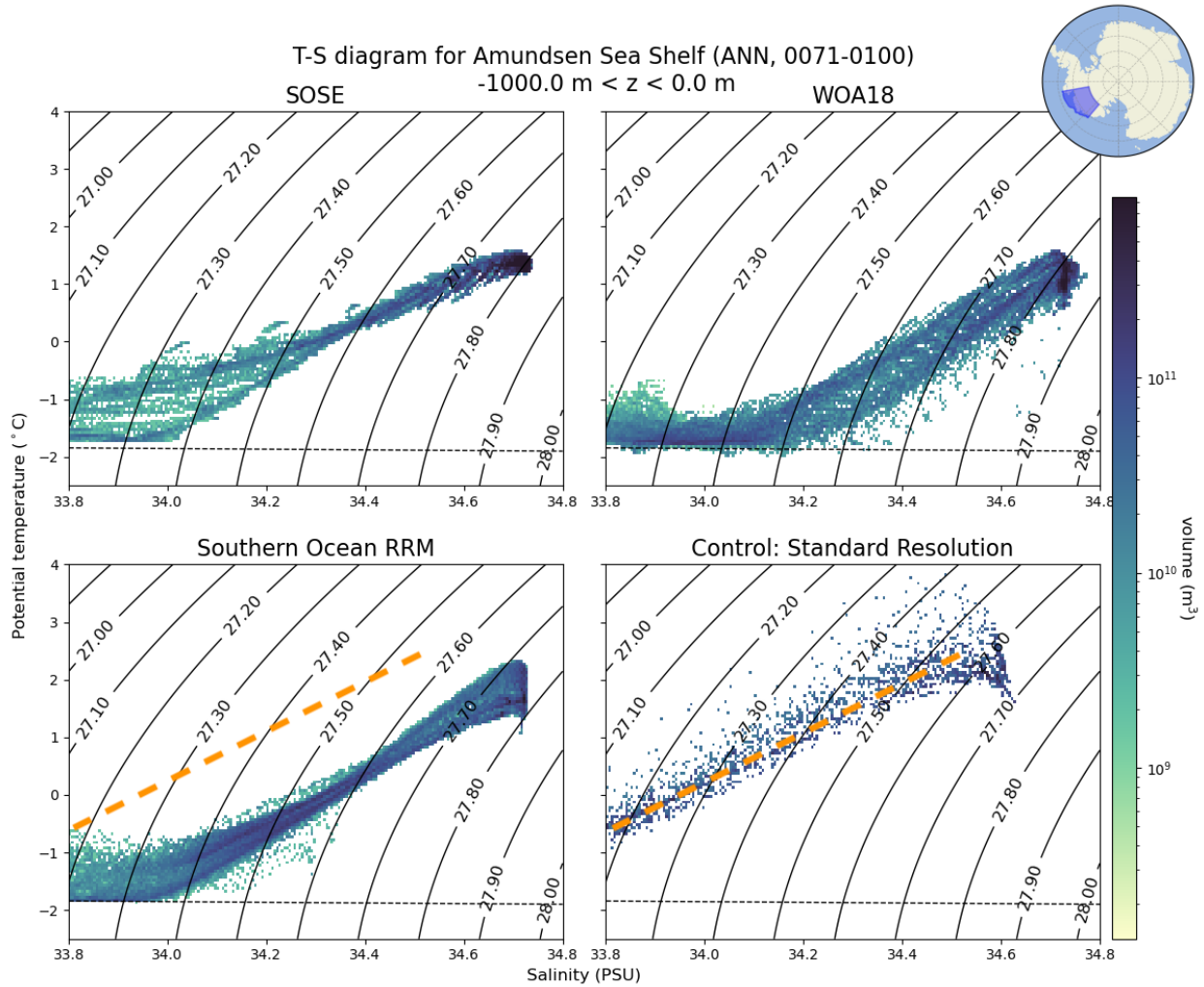


Figure 14. Temperature and salinity diagrams for the Amundsen Sea continental shelf region, representative of Abbot Ice Shelf cavity conditions, from the following sources: World Ocean Atlas observations (WOA18; Boyer et al. 2018) (upper right); Southern Ocean State Estimate (SOSE; Mazloff 2010) (upper left); SORRM simulation (lower left); standard-resolution simulation (lower right). For the E3SM simulations, results are averaged over the last 30 years of a 100-year simulation. The dashed orange line in the bottom two plots, which is identically located, more clearly highlights how much fresher and warmer the standard-resolution values are relative to the SORRM values.

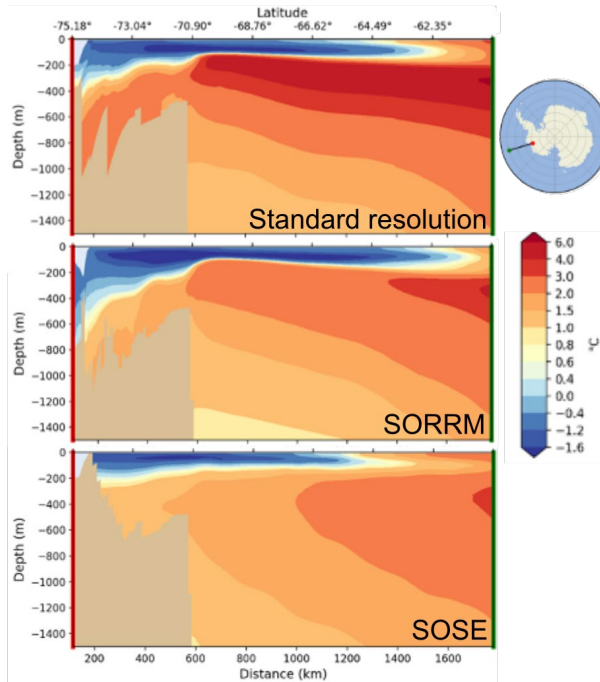


Figure 15. Modeled ocean temperatures along a transect in the Amundsen Sea region (inset figure at upper right) averaged over the last 30 years of our 100-year simulations. Shown are results from E3SM’s standard configuration (top row), from the SORRM configuration (middle row), and from the Southern Ocean State Estimate (SOSE; Mazloff et al. 2010) (bottom row).

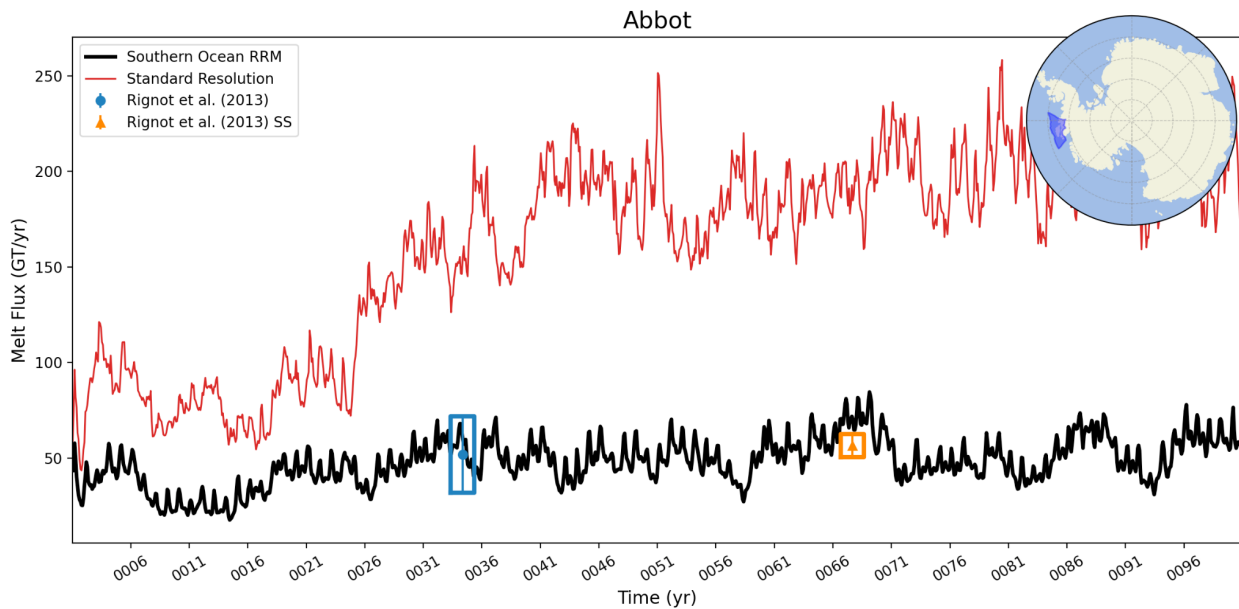


Figure 16. Time series of area-integrated, sub-ice-shelf melt flux for the Abbot Ice Shelf region of Antarctica. Melt fluxes from the standard-resolution and SORRM simulations are shown in red and black, respectively. The blue and orange boxes mark the span of melt rates inferred from observations of Rignot et al. (2013), with blue as an estimate for present-day and the orange an estimate for pre-industrial values (note that the position of the box along the horizontal axis is not relevant).

Filchner-Ronne Ice Shelf

The final region we discuss in detail is the Weddell Sea region and, in particular, the Filchner-Ronne Ice Shelf (FRIS), which is the largest ice shelf by volume in Antarctica. This region and ice shelf have been of interest to the broader ice sheet, ocean, and Earth system modeling communities for many years following initial studies suggesting that it could be vulnerable to a rapid mode switch, from cold to warm cavity circulation (e.g., Hellmer et al. 2012), whereby melt rates beneath the ice shelf can increase by more than an order of magnitude (e.g., Hellmer et al. 2017, Comeau et al. 2022). Multiple follow-on studies, including our own, have demonstrated this behavior and investigated its potential causes and implications (e.g., Hazel et al. 2020, Hoffman et al. 2022). Lower-resolution models (i.e., equivalent to the “standard”-resolution model here) may be overly sensitive to the conditions that allow for this mode switch (Bull et al. 2021). Because future projections that include such a switch will necessarily result in significantly higher amounts of sea level rise from Antarctica, it is critical to ensure that such a switch occurs for physically realistic reasons rather than as a result of model biases.

In Figures 16, 17, and 18, we show the same sets of regional plots and time series as for the other regions discussed above. The temperature and salinity diagram for the FRIS shows features common to those already discussed – namely, that cold and dense water, present in observations, is much better represented in our SORRM configuration than in our standard-resolution configuration. While there is still a bias towards being too fresh and too light in our SORRM configuration (i.e., HSSW is still mostly lacking), there are sufficiently dense waters on the continental shelf to keep warm, dense, off-shelf waters out of the cavity. A comparison of Weddell Sea continental shelf density profiles is shown in Figure 19, confirming that densities from the SORRM configuration are significantly and nearly everywhere denser than those from the standard configuration. It is the eventual inflow of these warm, dense waters that leads to the mode switch in cavity circulation and the extreme and rapid increase in sub-ice-shelf melt rates (Hoffman et al. 2022). While Figure 18 indicates that for century-scale simulations both the standard and SORRM configurations do a reasonable job of simulating FRIS melt fluxes, longer simulations with the standard configuration (not shown here) are prone to the triggering of this instability. Additional off-shelf warm biases in our standard configuration (Figure 17) would further exacerbate this problem.

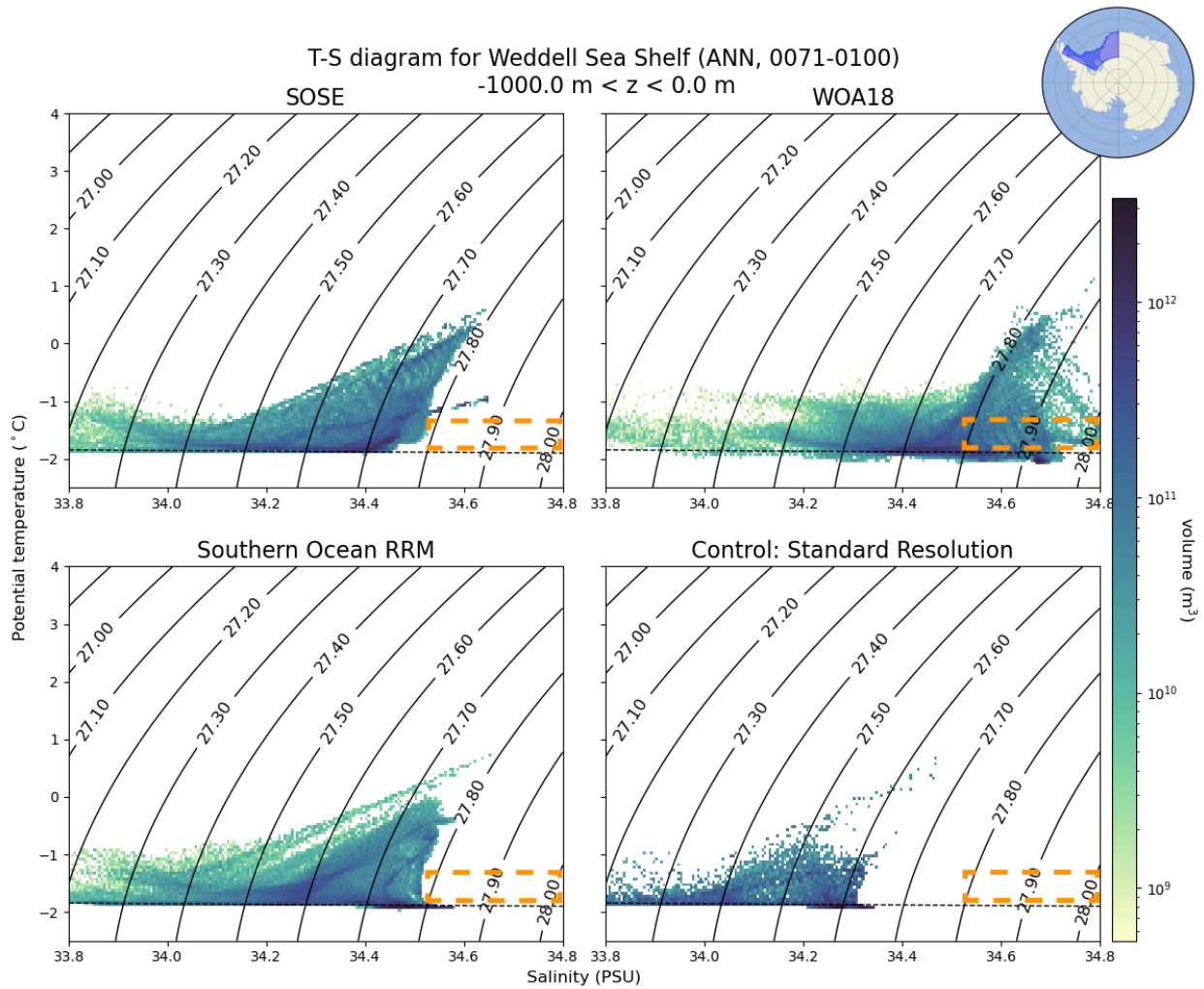


Figure 17. Temperature and salinity diagrams for the Weddell Sea continental shelf region, representative of Filchner-Ronne Ice Shelf cavity conditions, from the following sources: World Ocean Atlas observations (WOA18; Boyer et al. 2018) (upper right); Southern Ocean State Estimate (SOSE; Mazloff 2010) (upper left); SORRM simulation (lower left); standard-resolution simulation (lower right). For the E3SM simulations, results are averaged over the last 30 years of a 100-year simulation. The orange dashed box marks the region in temperature, salinity, and density space representative of high-salinity shelf water (HSSW).

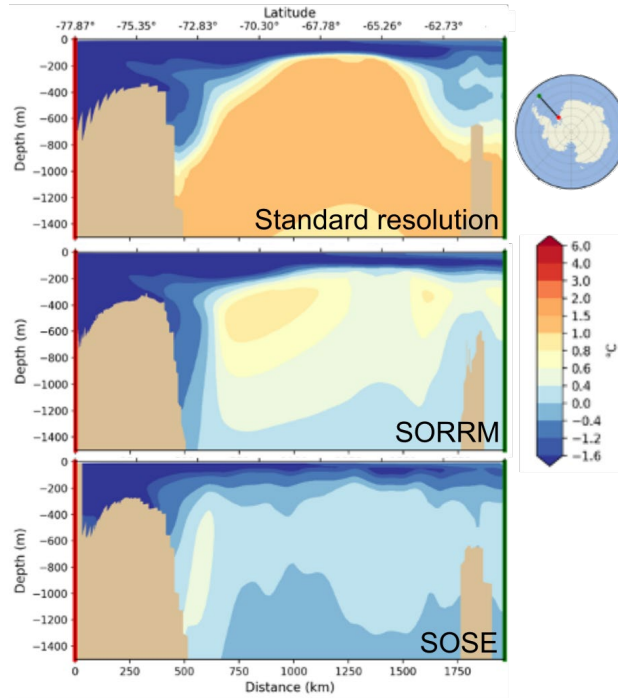


Figure 18. Modeled ocean temperatures along a transect in the Weddell Sea region, through the Filchner-Ronne Ice Shelf (inset figure at upper right) averaged over the last 30 years of our 100-year simulations. Shown are results from E3SM’s standard configuration (top row), from the SORRM configuration (middle row), and from the Southern Ocean State Estimate (SOSE; Mazloff et al. 2010) (bottom row).

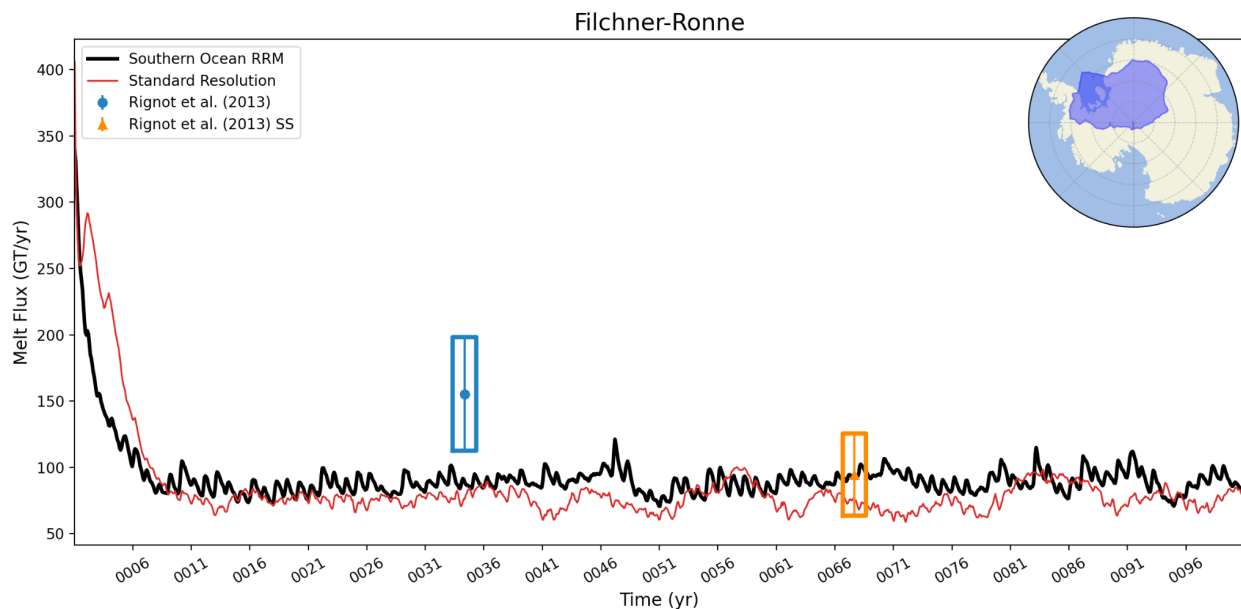


Figure 19. Time series of area-integrated, sub-ice-shelf melt flux for the Filchner-Ronne Ice Shelf region of Antarctica. Melt fluxes from the standard-resolution and SORRM simulations are shown in red and black, respectively. The blue and orange boxes mark the span of melt rates inferred from observations of Rignot et al. (2013), with blue as an estimate for present-day and orange an estimate for pre-industrial values (note that the position of the box along the horizontal axis is not relevant).

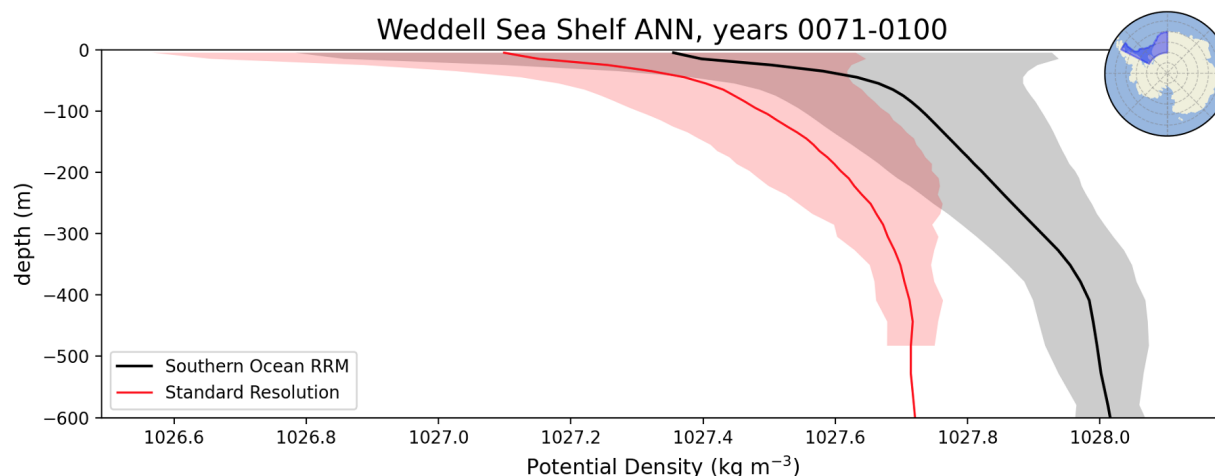


Figure 20. Comparison of Weddell Sea continental shelf density profiles for the standard configuration (red) and the SORRM configuration, averaged over the last 30 years of the simulations. Shading represents the range of values and the solid lines represent the averages.

4.0 References

- Boyer, TP, HE Garcia, RA Locarnini, MM Zweng, AV Mishonov, JR Reagan, KA Weathers, OK Baranova, D Seidov, and IV Smolyar, eds. 2018. *World Ocean Atlas 2018*; “Temperature” in Vol. 1 and “Salinity” in Vol. 2. NOAA Atlas NESDIS. <https://www.ncei.noaa.gov/products/world-ocean-atlas>
- Brondex, J, F Gillet-Chaulet, and O Gagliardini. 2019. “Sensitivity of centennial mass loss projections of the Amundsen basin to the friction law.” *The Cryosphere* 13(1): 177–195, <https://doi.org/10.5194/tc-13-177-2019>
- Bull, CYS, A Jenkins, NC Jourdain, I Vankova, PR Holland, P Mathiot, U Hausmann, and J-B Sallee. 2021. “Remote Control of Filchner-Ronne Ice Shelf Melt Rates by the Antarctic Slope Current.” *Journal of Geophysical Research: Oceans* 126(2): e2020JC016550, <https://doi.org/10.1029/2020JC016550>
- Comeau, D, XS Asay-Davis, CB Begeman, MJ Hoffman, W Lin, MR Petersen, SF Price, AF Roberts, LP Van Roekel, M Veneziani, JD Wolfe, JG Fyke, TD Ringler, and AK Turner. 2022. “The DOE E3SM v1.2 Cryosphere Configuration: Description and Simulated Antarctic Ice-Shelf Basal Melting.” *Journal of Advances in Modeling Earth Systems* 14(2) 1–25, <https://doi.org/10.1029/2021ms002468>
- Dinniman, M, XS Asay-Davis, BK Galton-Fenzi, PR Holland, A Jenkins, and R Timmermann. 2016. “Modeling Ice Shelf/Ocean Interaction in Antarctica: A Review.” *Oceanography* 29(4): 144–153, <https://doi.org/10.5670/oceanog.2016.106>
- Gent, PR, and JC McWilliams. 1990. “Isopycnal mixing in ocean circulation models.” *Journal of Physical Oceanography* 20(1): 150–155, [https://doi.org/10.1175/1520-0485\(1990\)020<0150:IMIOCM>2.0.CO;2](https://doi.org/10.1175/1520-0485(1990)020<0150:IMIOCM>2.0.CO;2)

- Gudmundsson, GH. 2013. “Ice-shelf buttressing and the stability of marine ice sheets.” *Cryosphere* 7(2): 647–655, <https://doi.org/10.5194/tc-7-647-2013>
- Hazel, JE, and AL Stewart. 2020. “Bistability of the Filchner-Ronne Ice Shelf Cavity Circulation and Basal Melt.” *Journal of Geophysical Research: Oceans* 125(4): 1–21, <https://doi.org/10.1029/2019JC015848>
- Hellmer, HH, F Kauker, R Timmermann, J Determann, and J Rae. 2012. “Twenty-first-century warming of a large Antarctic ice-shelf cavity by a redirected coastal current.” *Nature* 485(7397): 225–228, <https://doi.org/10.1038/nature11064>
- Hellmer, HH, F Kauker, R Timmermann, and T Hattermann. 2017. “The fate of the Southern Weddell sea continental shelf in a warming climate.” *Journal of Climate* 30(12): 4337–4350, <https://doi.org/10.1175/JCLI-D-16-0420.1>
- Hoffman, MJ, et al. 2022. “Characteristics of a tipping point in ice-shelf melt beneath the Filchner-Ronne Ice Shelf, Antarctica in a CMIP class ocean model.” *Ocean Modeling* (in prep).
- Heuzé, C, KJ Heywood, DP Stevens, and JK Ridley. 2013. “Southern Ocean bottom water characteristics in CMIP5 models.” *Geophysical Research Letters* 40(7): 1409–1414, <https://doi.org/10.1002/grl.50287>
- Jeong, H, XS Asay-Davis, AK turner, DS Comeau, SF Price, RP Abernathy, M Veneziani, MR Petersen, MJ Hoffman, MR Mazloff, and TD Ringler. 2020. “Impacts of ice-shelf melting on water-mass transformation in the Southern Ocean from E3SM simulations.” *Journal of Climate* 33(13): 5787–5807, <https://doi.org/10.1175/JCLI-D-19-0683.1>
- Li, G, J Guo, L Pei, S Zhang, X Tang, and J Yao. 2021. “Extraction and Analysis of the Three-Dimensional Features of Crevasses in the Amery Ice Shelf Based on ICESat-2 ATL06 Data.” *IEEE Journal of Selected Topics in Applied Earth Observations and Remote Sensing* 14: 5796–5806, <https://doi.org/10.1109/JSTARS.2021.3085302>
- Li, X, W Cai, GA Meehl, D Chen, X Yuan, M Raphael, DM Holland, Q Ding, RL Fogt, BR Markle, G Wang, DH Bromwich, J Turner, S-P Xie, EJ Steig, ST Gille, C Xiao, B Wu, MA Lazzara, X Chen, S Stammerjohn, PR Holland, MM Holland, X Cheng, SF Price, Z Wang, CM Bitz, J Shi, EP Gerber, X Liang, H Goosse, C Yoo, M Ding, L Geng, M Xin, C Li, T Dou, C Liu, W Sun, X Wang, and C Song. 2021. “Tropical teleconnection impacts on Antarctic climate changes.” *Nature Reviews Earth & Environment* 2: 680–698, <https://doi.org/10.1038/s43017-021-00204-5>
- Makinson, K, MA King, KW Nicholls, and GH Gudmundsson. 2012. “Diurnal and semidiurnal tide-induced lateral movement of Ronne Ice Shelf, Antarctica.” *Geophysical Research Letters* 39(10), L10501, <https://doi.org/10.1029/2012GL05163>
- Mazloff, MR, P Heimbach, and C Wunsch. 2010. “An Eddy-Permitting Southern Ocean State Estimate.” *Journal of Physical Oceanography* 40(5): 880–899. <https://doi.org/10.1175/2009JPO4236>
- Pattyn, F, and M Morlighem. 2020. “The uncertain future of the Antarctic Ice Sheet.” *Science* 367(6484): 1331–1335, <https://doi.org/10.1126/science.aaz5487>

Rignot, E, S Jacobs, J Mouginot, and B Scheuchl. 2013. “Ice-Shelf Melting Around Antarctica.” *Science* 341(6143): 266–270, <https://doi.org/10.1126/science.1235798>

Russell, JL, I Kamenkovich, C Bitz, R Ferrari, ST Gille, PJ Goodman, R Hallberg, K Johnson, K Khazmutdinova, I Marinov, M Mazloff, S Riser, JL Sarmiento, K Speer, LD Talley, and R Wanninkhof. 2018. “Metrics for the evaluation of the Southern Ocean in coupled climate models and earth system models.” *Journal of Geophysical Research: Oceans* 123(5): 3120–3143, <https://doi.org/10.1002/2017JC013461>

Scambos, TA, JA Bohlander, CA Shuman, and P Skvarca. 2004. “Glacier acceleration and thinning after ice shelf collapse in the Larsen B embayment, Antarctica.” *Geophysical Research Letters* 31(18): L18402, <https://doi.org/10.1029/2004GL020670>

Schmidtko, S, KJ Heywood, AF Thompson, and S Aoki. 2014. “Multidecadal warming of Antarctic waters.” *Science* 346(6214): 1227–1231, <https://doi.org/10.1126/science.1256117>

Sun, S, F Pattyn, EG Simon, T Albrecht, S Cornford, R Calov, C Dumas, F Gillet-Chaulet, H Goelzer, NR Golledge, R Greve, MJ Hoffman, A Humbert, E Kazmierczak, T Kleiner, GR Leguy, WH Lipscomb, D Martin, M Morlighem, S Nowicki, D Pollard, S Price, A Quiquet, H Seroussi, T Schlemm, J Sutter, RSW van de Wal, R Winkelmann, and T Zhang. 2020. “Antarctic ice sheet response to sudden and sustained ice-shelf collapse (ABUMIP).” *Journal of Glaciology* 66(260): 891–904, <https://doi.org/10.1017/jog.2020.67>

Talley, L. 2011. *Descriptive Physical Oceanography*. 6th edition. Academic Press, ISBNL: 9780750645522, <https://doi.org/10.1016/C2009-0-24322-4>

Thompson, AF, AL Stewart, P Spence, and KJ Heywood. 2018. “The Antarctic Slope Current in a Changing Climate.” *Reviews of Geophysics* 56(4): 741–770, <https://doi.org/10.1029/2018RG000624>

Veneziani, M, et al. 2019. “The Antarctic Slope Current (ASC) and cross-shelf circulation in E3SMv1 simulations.” *E3SM Spring All Hands Meeting*, March 20, 2019.



U.S. DEPARTMENT OF
ENERGY

Office of Science